galaxies

MDPI

Article

Ultra Light Axionic Dark Matter: Galactic Halos and Implications for Observations with Pulsar Timing Arrays

Ivan de Martino [1,*], Tom Broadhurst [1,2], S.-H. Henry Tye [3], Tzihong Chiueh [4], Hsi-Yu Schive [5] and Ruth Lazkoz [1]

1 Department of Theoretical Physics, University of the Basque Country UPV/EHU, E-48080 Bilbao, Spain; tom.j.broadhurst@gmail.com (T.B.); ruth.lazkoz@ehu.eus (R.L.)
2 Ikerbasque, Basque Foundation for Science, E-48011 Bilbao, Spain
3 Institute for Advanced Study and Department of Physics, Hong Kong University of Science and Technology, Hong Kong, China; iastye@ust.hk
4 National Center for Theoretical Sciences, National Taiwan University, Taipei 10617, Taiwan; chiuehth@phys.ntu.edu.tw
5 National Center for Supercomputing Applications, Urbana, IL 61801, USA; hyschive@gmail.com
* Correspondence: ivan.demartino@ehu.eus

Received: 29 November 2017; Accepted: 8 January 2018; Published: 16 January 2018

Abstract: The cold dark matter (CDM) paradigm successfully explains the cosmic structure over an enormous span of redshifts. However, it fails when probing the innermost regions of dark matter halos and the properties of the Milky Way's dwarf galaxy satellites. Moreover, the lack of experimental detection of Weakly Interacting Massive Particle (WIMP) favors alternative candidates such as light axionic dark matter that naturally arise in string theory. Cosmological N-body simulations have shown that axionic dark matter forms a solitonic core of size of $\simeq$150 pc in the innermost region of the galactic halos. The oscillating scalar field associated to the axionic dark matter halo produces an oscillating gravitational potential that induces a time dilation of the pulse arrival time of $\simeq$400 ns/($m_B/10^{-22}$ eV) for pulsar within such a solitonic core. Over the whole galaxy, the averaged predicted signal may be detectable with current and forthcoming pulsar timing array telescopes.

Keywords: dark matter; axions; particle physics; general relativity; pulsars; SKA

1. Introduction

One of the biggest challenges to modern cosmology and astrophysics is the understanding of how galaxies and clusters of galaxies formed and evolved. In the context of general relativity, it is well known that observations of the large-scale structure of the Universe cannot be explained without assuming the existence of a dark matter component that can be classified, according to its characteristic free-streaming length, into: hot (with the particle's mass on the eV scale); warm (with the mass on the keV scale) and, finally, cold (with mass on the GeV scale). Only cold dark matter (CDM) is able to account for the observed large-scale structure of the Universe. Thus, the CDM paradigm has become one of the fundamental pillars of the standard cosmological model.

Although the existence of dark matter is observationally well-established, its nature and particle properties are still unknown [1,2]. Over the last decades, cosmological N-body simulations have increased their resolution, allowing the internal structure of CDM halos on small scales to be resolved. Thus, several challenges for the CDM paradigm emerged. First, there is the "cuspy-core problem": N-body simulations predicted that the central density increases as $r^{-\beta}$ with $\beta \sim$1–1.5, while observations of dark matter-dominated systems, such as low surface brightness (LSB) galaxies and

dwarf spheroidal (dSph) galaxies, suggest a constant density profile in the innermost regions of the halos. Second, there is the "missing satellite problem": simulations predict an overabundance of substructures within the dark matter halos compared with high-resolution observations. Third, there is the "too-big-to-fail" problem: Milky Way satellites are not massive enough to be consistent with CMD predictions. Finally, another potential difficulty may lie in the early formation of large galaxies: large systems are formed hierarchically through the merging of small galaxies that collapsed earlier, but recent observations have found various massive galaxies at very high redshifts; it remains to be seen whether such rapid formation could represent a problem for the CDM model (for comprehensive reviews see [3] and references within).

Many possible solutions to the above issues have been proposed. First, N-body simulations of dwarf galaxies in the CDM model that include a bursty and continuous star formation rate show a flat density profile in the innermost region. However, the "cusp-core problem" still exists for low mass galaxies ($\leq 10^{6.5} M_{\odot}$) and in some LSB galaxies. Second, some empirical profiles such as the Burkert profile, or the generalized Navarro-Frenk-White (NFW) profile have been proposed, but they lack of theoretical support. Third, there are some modified gravity models capable of reproducing the observations of galaxy clusters and they are also consistent with data at the galactic level [4–9]. Finally, alternative candidates to the CDM paradigm, such as scalar field dark matter and others, have been proposed [10–19].

Such scalar fields naturally arise in string theory and many of them contain an axionic mode that is massless during the hot big bang epoch [20–23]. The wave nature of light scalar dark matter, with only the boson mass as free parameter, has been shown to be capable of resolving some small-scale problems [24]. Here we consider ultralight scalar fields with masses $m_B = 10^{-23} - 10^{-22}$ eV that can naturally emerge in this context [25,26]. Ultralight scalar field dark matter is able to solve both the "cuspy-core" and the "missing satellites" problems [27,28]. This is well described by a oscillating classical scalar field with frequency m_B that leads to an oscillating pressure field with frequency $2m_B$, which averages to zero on time scales much larger than $1/m_B$. Such a Compton oscillation leads to an oscillating gravitational potential which could produce a timing shift in the pulsar timing measurements [29] opening up the possibility of detecting an imprint of scalar field dark matter with the next generation of radio telescope and Pulsar Timing Array (PTA) experiments.

Here, we have summarized our contributions to the comprehension of the effect produced by axionic dark matter on the pulsar timing measurements [30]. In Section 2 we summarize the main astrophysical features of the scalar field dark matter model; in Section 3, we write down the equations to compute timing shift in the pulsar timing measurements; in Section 4, we show the main results; and, finally, in Section 5, we present the conclusions.

2. The ψ-Dark Matter Halo

Forms of scalar field dark matter, such as axions, if sufficiently light, can satisfy the ground state condition that can be described by a coupled Schrödinger–Poisson equations in comoving coordinates [31]:

$$\left[i\frac{\partial}{\partial \tau} + \frac{\nabla^2}{2} - aV \right] \psi = 0\,, \tag{1}$$

$$\nabla^2 V = 4\pi(|\psi|^2 - 1)\,. \tag{2}$$

Here, ψ is the wave function, V is the gravitation potential, and a is the cosmological scale factor. The system is normalized to the time scale $d\tau = \chi^{1/2} a^{-2} dt$, and to the scale length $\tilde{\xi} = \chi^{1/4} (m_B/\hbar)^{1/2} \mathbf{x}$, where $\chi = \frac{3}{2} H_0^2 \Omega_0$ and m_B indicates the particle mass, while H_0 and Ω_0 represent the present Hubble and dark matter density parameters.

Pioneering high resolution cosmological simulation of this wavelike dark matter (ψDM) has been capable of revealing unpredicted small-scale structures on the de Broglie scale. Employing only one

free parameter, the boson mass (m_B), the ψDM model predicts the formation of solitonic cores in the innermost region of each virialized halo, which accounts for the dark matter-dominated cores of dwarf spheroidal galaxies [27]. Moreover, the central soliton is surrounded by an extended halo showing a granular texture on the de Broglie scale [32]. The functional form of the soliton density profile can be well approximated by

$$\rho_c(x) \sim \frac{1.9\, a^{-1}(m_B/10^{-23}\,\mathrm{eV})^{-2}(x_c/\mathrm{kpc})^{-4}}{[1+9.1\times10^{-2}(x/x_c)^2]^8}\, M_\odot \mathrm{pc}^{-3}. \tag{3}$$

while it is, when azimuthally averaged, indistinguishable from the well known NFW profile in the outermost region of the galaxy.

Since the occupation number of dark matter particle in the galactic halo is enormous [29]

$$\frac{\Delta N}{\Delta x^3 \Delta k^3} \gtrsim \frac{\rho_{DM}}{m_B}\lambda_{dB}^3 \sim 10^{95}\,, \tag{4}$$

dark matter can be well described by a classical oscillating scalar field $\phi(\mathbf{x},t)$ with Compton frequency $\omega_B = (2.5\,\mathrm{months})^{-1}(m_B/10^{-22}\,\mathrm{eV})$:

$$\phi(\mathbf{x},t) = A(\mathbf{x})\cos(\omega_B\, t + \alpha(\mathbf{x})). \tag{5}$$

The energy-momentum tensor associated to this scalar field is given by

$$T_{\mu\nu} = \partial_\mu\phi\partial_\nu\phi - \frac{1}{2}g_{\mu\nu}[(\partial\phi)^2 - m_B^2\phi^2]\,, \tag{6}$$

and the time-independent energy density is

$$\rho_{DM}(\mathbf{x}) = \frac{1}{2}[\dot{\phi}^2 + m_B^2\phi^2 + (\nabla\phi)^2] \approx \frac{1}{2}m_B^2 A(\mathbf{x})^2\,. \tag{7}$$

Finally, the pressure field is given by

$$p(\mathbf{x},t) = \frac{1}{2}[\dot{\phi}^2 - m_B^2\phi^2 - (\nabla\phi)^2] \approx -\frac{1}{2}m_B^2 A(\mathbf{x})^2 cos(2\omega_B t + 2\alpha(\mathbf{x}))\,, \tag{8}$$

and, although averaged over period pressure is zero, oscillations induce time-dependent gravitational potential on the de Broglie scales.

3. Shift of the Pulse Arrival Time

The starting point to compute such oscillating gravitation potential is to write down the halo metric in the Newtonian gage

$$ds^2 = (1+2\Phi(\mathbf{x},t))dt^2 - (1-2\Psi(\mathbf{x},t))\delta_{ij}dx_i dx_j\,, \tag{9}$$

then, the gravitational potentials $\Phi(\mathbf{x},t)$ and $\Psi(\mathbf{x},t)$ can be computed linearizing the Einstein equations and recasting the two potentials as the sum of a dominant time-independent part and small oscillating part

$$\Psi(\mathbf{x},t) \simeq \Psi_0(\mathbf{x}) + \Psi_c(\mathbf{x})cos(\omega_B t + 2\alpha(\mathbf{x})) + \Psi_s(\mathbf{x})sin(\omega_B t + 2\alpha(\mathbf{x}))\,. \tag{10}$$

The time-independent part can be computed from the time component, while the oscillating part is computed from the trace of the spatial components of the field equations [29]:

$$\Delta\Psi(\mathbf{x},t) = 4\pi G\rho_{DM}(\mathbf{x})\,, \tag{11}$$

$$-6\ddot{\Psi}(\mathbf{x},t) + 2\Delta(\Psi(\mathbf{x},t) - \Phi(\mathbf{x},t)) = 24\pi G p(\mathbf{x},t)\,, \tag{12}$$

form which one obtains

$$\Psi_c(\mathbf{x}) = \frac{1}{2}\pi G A(\mathbf{x})^2 \equiv \pi \frac{G\rho_{DM}(\mathbf{x})}{m_B^2}\,, \tag{13}$$

$$\Psi_s(\mathbf{x}) = 0\,. \tag{14}$$

Any propagating signal is affected by such time-dependent potential. When considering ultralight scalar fields, the gravitational potential oscillates with a frequency $2m_B$ that lies in the range of PTA experiments [33]. The main effect is a shift in the pulse arrival times of a pulsar population. When a pulse is modeled, many astrophysical and kinematic effects must be taken into account [34]. Thus, the residuals can be ascribed to other effects such as the emission of gravitational waves or the axionic dark matter halo. These time residuals can be modeled as the relative frequency shift of the pulse

$$\delta t(t) = -\int_0^t \frac{\nu(t') - \nu_0}{\nu_0}\, dt'\,, \tag{15}$$

where $\nu(t)$ is the frequency of the pulse at the detector at the time t, and ν_0 is the pulse emission frequency at the pulsar. Considering the linearized Einstein equations in the Newtonian gauge, the frequency shift can be recast as [35]

$$\frac{\nu(t) - \nu_0}{\nu_0} \approx \Psi(\mathbf{x_p}, t_0) - \Psi(\mathbf{x}, t)\,. \tag{16}$$

Since the amplitude of the oscillation of the gravitational potential will vary on the sky as the density of dark matter in the galaxy, the time-dependent part of the time residuals for the $i-th$ pulsar can be written as

$$\Delta t_i(t) = \frac{1}{\omega_B}\left[\Psi(\mathbf{x_i})\sin\left(\omega_B t - \frac{\omega_B D_i}{c} + 2\alpha_i\right) - \Psi(\mathbf{x_e})\sin\left(\omega_B t + 2\alpha_e\right)\right], \tag{17}$$

where $\alpha_i \equiv \alpha(\mathbf{x_i})$ and D_i are the phase and the distance to the i-th pulsar, respectively, and $\alpha_e \equiv \alpha(\mathbf{x_e})$ is the phase of the Earth clock.

In order to maximize the effect of the oscillating gravitational potential and avoid the same dependence of Earth clocks on the local density of axionic matter, we may study the difference of the time residuals between two pulsars. The relative timing amplitudes for pairs of pulsars $S(t)$ [30] is:

$$S(t) = \Delta t_1(t) - \Delta t_2(t) = \frac{1}{\omega_B}\left[\Psi(\mathbf{x_1})\sin\left(\omega_B t + \alpha_1'\right) - \Psi(\mathbf{x_2})\sin\left(\omega_B t + \alpha_2'\right)\right], \tag{18}$$

where we have defined $\alpha_i' = 2\alpha_i - \frac{\omega_B D_i}{c}$ with $i = \{1, 2\}$.

Finally the characteristic amplitude associated to the oscillating gravitational potential was computed by averaging the square signal over all the phases of a pulsar population

$$h_c^{SF} = \frac{\sqrt{6}}{2}\Psi(\mathbf{x_2})\sqrt{1 + \delta\rho_{DM}^2}\,, \tag{19}$$

where

$$\delta\rho_{DM} = \left(\frac{\Psi(\mathbf{x_1})}{\Psi(\mathbf{x_2})}\right) = \frac{\rho_{DM}(\mathbf{x_1})}{\rho_{DM}(\mathbf{x_2})}. \tag{20}$$

Here, $\Psi(\mathbf{x_2})$ can be written in terms of $\Psi(\mathbf{x_1})$ because the amplitude of the oscillations only depends on the dark matter density distribution.

4. Results

The amplitudes of the predicted residuals due to the oscillating gravitational potential are illustrated in Figure 1 with the boson mass fixed to $m_B \sim 0.8 \times 10^{-22}$ eV. The figure is particularized

to show the relative timing signal between local pulsars at 8 kpc, and pulsars close to the galactic center at a radius of 50 and 500 pc. The most important case is represented in top-left panel where the amplitude of the residuals, that is dominated by the pulsar closer to the galactic center, reaches $\sim$ 600 ns. Pulsars located at higher distance from the center give rise to a smaller effect that reaches the order of $\sim$ns for local pulsars (as already predicted in [29]). In the bottom left and right panels both pulsars are located at the same galactocentric radius of 0.5 and 8 kpc, respectively. In this case, the predicted amplitude of the residuals strongly depends on the phase of the pulse. The light red shaded regions indicate how the density fluctuations of the dark matter distribution, that give rise to the granular texture shown in [27], enhance or reduce the relative timing signal depending whether the pulsar is located in higher or lower density region with respect the average distribution.

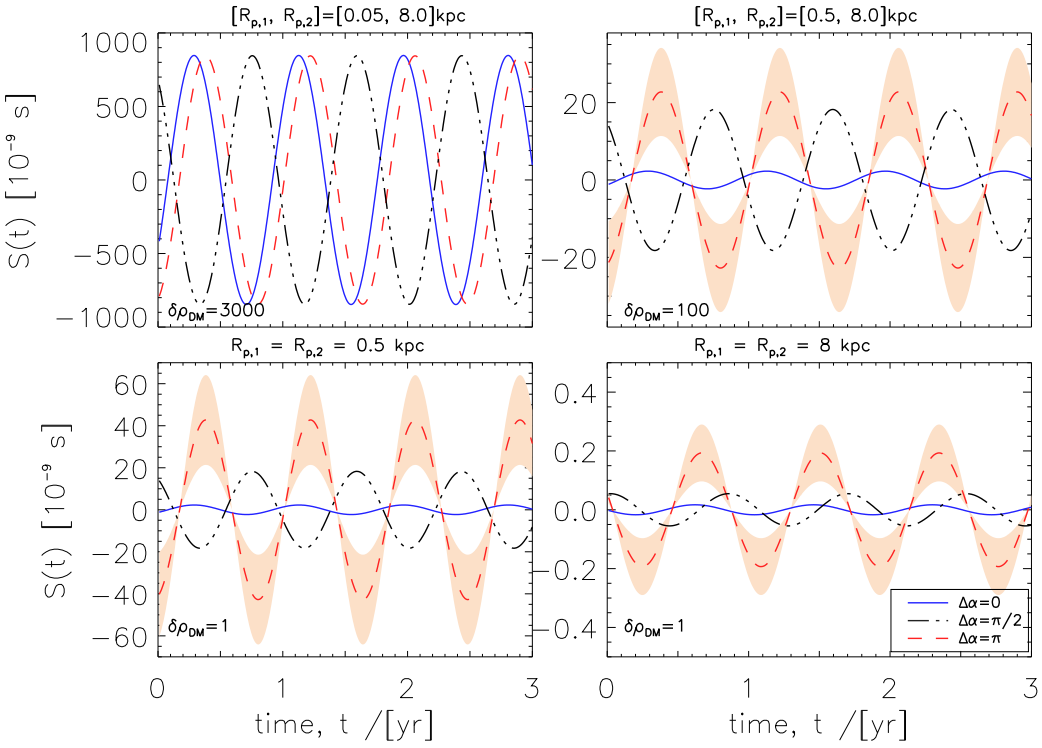

Figure 1. The plot shows the predicted timing signal between pulsar pairs, for a light scalar field of $m_B \sim 0.8 \times 10^{-22}$ eV.

Figure 2 shows the characteristic amplitude predicted between pairs of pulsars and a comparison with sensitivity of the current and forthcoming PTA detectors. Pairs of pulsars are located at the same galactocentric distances chosen in Figure 1. The characteristic amplitude has been computed for pulsars within the galactic soliton region as function of the boson mass. The signal could be already detectable for pulsars near the galactic center. For comparison, the diagonal dotted line is the predicted amplitude obtained by [29] for local pulsars. The green shaded region represents the predicted range of the signal due to the granular modulation. Finally, the black square indicates the local upper limit obtained by [36].

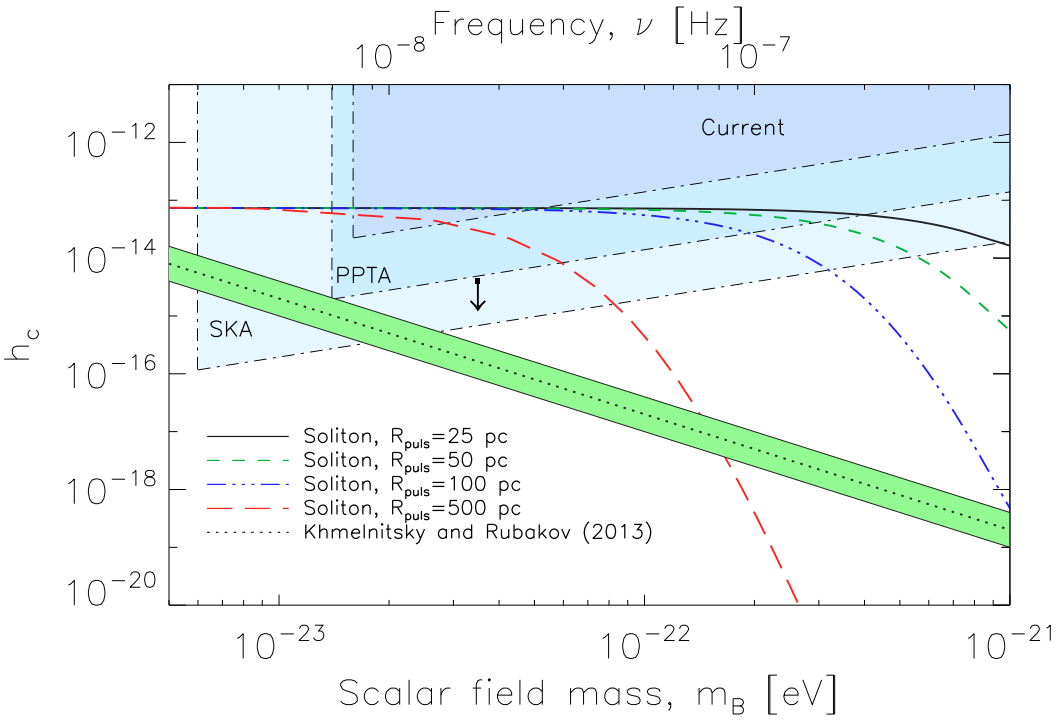

Figure 2. The characteristic strain measured between pairs of pulsars is shown. It is compared with the expected sensitivities from the current and forthcoming PTA experiments (adapted from [29,37]).

5. Discussion and Conclusions

The axionic dark matter halo can be described as a classical oscillating scalar field. Such a field generates an oscillating gravitational potential that affects the pulsar timing signal. Although the amplitude of such an effect is comparable to that expected from the stochastic gravitational wave background, it is isotropic and has a characteristic frequency scale. In the model developed in [29] we have implemented the characteristic features of the axionic dark matter density profile described in Section 2. We have shown that the amplitude of a signal emitted from pulsars near the galactic center can reach the order of hundreds of ns. Also, we have highlighted how the Compton modulation out of the solitonic region (the granularity feature) can enhance or reduce the signal depending on the phases of the two pulsars. Finally, we have shown that the averaged signal from pairs of pulsars can be related to the characteristic gravitational wave strain, and it may be detectable using current PTA detectors once pulsars within 150 kpc of the galactic center are discovered.

Acknowledgments: IDM acknowledges financial support from University of the Basque Country UPV/EHU under the program "Convocatoria de contratación para la especialización de personal investigador doctor en la UPV/EHU 2015", from the Spanish Ministerio de Economía y Competitividad through research project FIS2010-15492, and from the Basque Government through research project IT-956-16. RL is supported by the Spanish Ministry of Economy and Competitiveness through research projects FIS2010-15492 and Consolider EPI CSD2010-00064, and by the University of the Basque Country UPV/EHU under program UFI 11/55. IDM and RL also acknowledge support from the COST Action CA1511 Cosmology and Astrophysics Network for Theoretical Advances and Training Actions (CANTATA). TJB acknowledges generous hospitality from the Institute for Advanced Studies in Hong Kong and helpful conversations with Nick Kaiser and Kfir Blum. SHHT is supported by CRF Grant HKUST4/CRF/13G and GRF 16305414 issued by the Research Grants Council (RGC) of the Government of the Hong Kong SAR. Chipbond Technology Corporation is acknowledged for donating the GPU cluster with which this work was conducted. This work was supported in part by the National Science Council of Taiwan under grants NSC100-2112-M-002-018-MY3 and NSC99-2112-M-002-009-MY3.

Author Contributions: All authors equally contributed to the paper.

Conflicts of Interest: The authors declare no conflict of interest.

References

1. Bertone, G.; Hooper, D.; Silk, J. Particle dark matter: Evidence, candidates and constraints. *Phys. Rep.* **2005**, *405*, 279.
2. Feng, J.L. Dark Matter Candidates from Particle Physics and Methods of Detection. *Ann. Rev. Astron. Astrophys.* **2008**, *48*, 495.
3. Bullock, J.S.; Boylan-Kolchin, M. Small-Scale Challenges to the ΛCDM Paradigm. *Ann. Rev. Astron. Astrophys* **2017**, *55*, 343–387.
4. Capozziello, S.; De Laurentis, M. Extended Theories of Gravity. *Phys. Rep.* **2011**, *509*, 167.
5. Capozziello, S.; De Laurentis, M. The dark matter problem from $f(R)$ gravity viewpoint. *Ann. Phys.* **2012**, *524*, 545.
6. De Martino, I.; De Laurentis, M.; Atrio-Barandela, F.; Capozziello, S. Constraining f(R) gravity with Planck data on galaxy cluster profiles. *Mon. Not. R. Astron. Soc.* **2014**, *442*, 921–928.
7. De Martino, I.; De Laurentis, M.; Capozziello, S. Constraining $f(R)$ gravity by the Large Scale Structure. *Universe* **2015**, *1*, 123.
8. De Martino, I. $f(R)$-gravity model of the Sunyaev-Zeldovich profile of the Coma cluster compatible with Planck data. *Phys. Rev. D* **2016**, *93*, 124043.
9. De Martino, I.; De Laraurentis, M. On the universality of MOG weak field approximation at galaxy cluster scale. *Phys. Lett. B* **2017**, *770*, 440.
10. Berezhiani, Z.G.; Khlopov, M.Y. Cosmology of spontaneously broken gauge family symmetry with axion solution of strong CP-problem. *Z. Phys. C Part. Fields* **1991**, *49*, 73–78.
11. Berezhiani, Z.G.; Sakharov, A.S.; Khlopov, M.Y. Primordial background of cosmological axions. *Sov. J. Nucl. Phys.* **1992**, *55*, 1063–1071.
12. Sakharov, A.S.; Khlopov, M.Y. The nonhomogeneity problem for the primordial axion field. *Phys. Atom. Nucl.* **1994**, *57*, 485–487.
13. Sakharov, A.S.; Sokoloff, D.D.; Khlopov, M.Y. Large scale modulation of the distribution of coherent oscillations of a primordial axion field in the Universe. *Phys. Atom. Nucl.* **1996**, *59*, 1005–1010.
14. Khlopov, M.Y.; Sakharov, A.S.; Sokoloff, D.D. The nonlinear modulation of the density distribution in standard axionic CDM and its cosmological impact. *Nucl. Phys. B Proc. Suppl.* **1999**, *72*, 105–109.
15. Mielke, E.W.; Vélez Pérez, J.A. Toroidal halos in a nontopological soliton model of dark matter. *Phys. Rev. D* **2007**, *75*, 043504.
16. Mielke, E.W.; Vélez Pérez, J.A. Axion condensate as a model for dark matter halos. *Phys. Lett. B* **2009**, *671*, 174–178.
17. Capolupo, A. Dark Matter and Dark Energy Induced by Condensates. *Adv. High Energy Phys.* **2016**, *2016*, 8089142.
18. Capolupo, A. Quantum vacuum, dark matter, dark energy and spontaneous supersymmetry breaking. *arXiv* **2017**, arXiv:1708.08769.
19. Capolupo, A. Cosmological Effects of Quantum Vacuum Condensates. *Galaxies* **2017**, *5*, 98.
20. Preskill, J.; Wise, M.B.; Wilczek, F. Cosmology of the Invisible Axion. *Phys. Lett. B* **1983**, *120*, 127.
21. Abbott, L.F.; Sikivie, P. A Cosmological Bound on the Invisible Axion. *Phys. Lett. B* **1983**, *120*, 133.
22. Dine, M.; Fischler, W. The Not So Harmless Axion. *Phys. Lett. B* **1983**, *120*, 137.
23. Svrcek, P.; Witten, E. Axions In String Theory. *J. High Energy Phys.* **2006**, *0606*, 051.
24. Hu, W.; Barkana, R.; Gruzinov, A. Cold and Fuzzy Dark Matter. *Phys. Rev. Lett.* **2000**, *85*, 1158.
25. Hui, L.; Ostriker, J.P.; Tremaine, S.; Witten, E. Ultralight scalars as cosmological dark matter. *Phys. Rev. D* **2017**, *95*, 043541.
26. Tye, S.-H.; Wong, S.S.C. Linking Light Scalar Modes with A Small Positive Cosmological Constant in String Theory. *J. High Energy Phys.* **2017**, *2017*, 94.
27. Schive, H.-Y.; Chiueh, T.; Broadhurst, T. Cosmic structure as the quantum interference of a coherent dark wave. *Nat. Phys.* **2014**, *10*, 496–499.
28. Schive, H.-Y.; Liao, M.-H.; Woo, T.-P.; Wong, S.-K.; Chiueh, T.; Broadhurst, T.; Pauchy Hwang, W.-Y. Understanding the Core-Halo Relation of Quantum Wave Dark Matter from 3D Simulations. *Phys. Rev. Lett.* **2014**, *113*, 261302.

29. Khmelnitsky, A.; Rubakov, V. Pulsar timing signal from ultralight scalar dark matter. *J. Cosmol. Astropart. Phys.* **2014**, *2014*, 019.
30. De Martino, I.; Broadhurst, T.; Tye, S.-H.H.; Chiueh, T.; Schive, H.-Y.; Lazkoz, R. Recognising Axionic Dark Matter by Compton and de-Broglie Scale Modulation of Pulsar Timing. *Phys. Rev. Lett.* **2017**, *119*, 221103.
31. Widrow, L.M.; Kaiser, N. Using the Schroedinger Equation to Simulate Collisionless Matter. *Astrophys. J.* **1993**, *416*, L71.
32. Woo, T.-P.; Chiueh, T. High-resolution simulation on structure formation with extremely light bosonic dark matter. *Astrophys. J.* **2009**, *697*, 850–861.
33. Moore, C.J.; Cole, R.H.; Berry, C.P.L. Gravitational-wave sensitivity curves. *Class. Quant. Grav.* **2015**, *32*, 015014.
34. Hobbs, G.; Jenet, F.; Lee, K.J.; Verbiest, J.P.W.; Yardley, D.; Manchester, R.; Lommen, A.; Coles, W.; Edwards, R.; Shettigara, C. TEMPO2, a new pulsar timing package. III: Gravitational wave simulation. *Mon. Not. R. Astron. Soc.* **2009**, *394*, 1945.
35. Gorbunov, D.S.; Rubakov, V.A. *Introduction to the Theory of the Early Universe*; World Scientific Pub. Co.: Singapore; Hackensack, NJ, USA, 2011.
36. Porayko, N.K.; Postnov, K.A. Constraints on ultralight scalar dark matter from pulsar timing. *Phys. Rev. D* **2014**, *90*, 062008.
37. Sesana, A.; Vecchio, A.; Colacino, C.N. The stochastic gravitational-wave background from massive black hole binary systems: Implications for observations with Pulsar Timing Arrays. *Mon. Not. R. Astron. Soc.* **2008**, *390*, 192–209.